High-Integrated-Photosensitivity Negative-Electron-Affinity GaAs Photocathodes with Multilayer Be-Doping Structures

Wang Xiaofeng[1], Zeng Yiping[1], Wang Baoqiang[1], Zhu Zhanping[1], Du Xiaoqing[2], Li Min[2], and Chang Benkang[2]

(1 *Institute of Semiconductors, Chinese Academy of Sciences, Beijing* 100083, *China*)
(2 *Institute of Electronic Engineering & Opto-Electronic Technology, Nanjing University of Science & Technology, Nanjing* 210094, *China*)

Abstract: The effect of changing Be doping concentration in GaAs layer on the integrated photosensitivity for negative-electron-affinity GaAs photocathodes is investigated. Two GaAs samples with the monolayer structure and the multilayer structure are grown by molecular beam epitaxy. The former has a constant Be concentration of 1×10^{19} cm^{-3}, while the latter includes four layers with Be doping concentrations of 1×10^{19}, 7×10^{18}, 4×10^{18}, and 1×10^{18} cm^{-3} from the bottom to the surface. Negative-electron-affinity GaAs photocathodes are fabricated by exciting the sample surfaces with alternating input of Cs and O in the high vacuum system. The spectral response results measured by the on-line spectral response measurement system show that the integrated photosensitivity of the photocathode with the multilayer structure enhanced by at least 50 % as compared to that of the monolayer structure. This attributes to the improvement in the crystal quality and the increase in the surface escape probability. Different stress situations are observed on GaAs samples with monolayer structure and multilayer structure, respectively.

Key words: integrated photosensitivity; multilayer structure; NEA photocathode; diffusion length; surface escape probability
PACC: 3365; 7000; 6000
CLC number: TN304.2+3 **Document code:** A **Article ID:** 0253-4177(2005)09-1692-07

1 Introduction

Negative-electron-affinity (NEA) GaAs photocathode has been developed rapidly since its discovery in 1960's due to its high quantum efficiency and good long-wavelength response[1,2]. The NEA surface refers to the condition that the vacuum level at the surface of a semiconductor lies below the conduction band minimum in the bulk. Therefore, the photoexcited electrons can diffuse to the narrow band-bending region of the activated surface, and traverse or tunnel through the interfacial potential spike with high probability. There have been several decades of experience with NEA photocathodes in night-vision applications[3,4]. Recently, Cs:O on (100) GaAs has become important as spin-polarized electron emitters[5].

To form an 'effective NEA' surface, a narrow band-bending region at the activated surface is required. Conventionally, highly doping concentration has been employed for GaAs photocathodes[1~4,6~8]. However, the corresponding decrease in the electron diffusion length will result in the deterioration of the spectral response.

To circumvent this problem, we adopt the idea of back surface field (BSF) structure[9] used in solar cells. In the BSF structure, there are two re-

Wang Xiaofeng female, PhD candidate. Her research interests include GaAs photo-cathode materials and devices. Email: xiaofw@red.semi.ac.cn

Received 21 February 2005, revised manuscript received 12 April 2005

gions with different concentrations. The potential energy barrier at the interface of the two regions tends to confine the minority carriers in the more lightly doped region away from the more heavily doped region. It is expected that the number of the photoelectrons diffused to the NEA surface should increase, and thus better photosensitivity should be obtained in NEA GaAs photocathode with such a BSF-like structure.

In this paper, we report on the fabrication of high-integrated-photosensitivity NEA GaAs photocathode with a multilayer structure. The crystal quality of the GaAs layer is characterized by photoluminescence (PL) and Raman spectroscopy. The spectral response properties of the photocathodes are determined using the on-line spectral response measurement system[10,11]. The results are compared with that of GaAs photocathode with a uniform structure.

2 Experiment

Two GaAs epitaxial samples on semi-insulating (SI) GaAs (100) substrates were grown by molecular beam epitaxy (MBE) under the same growth conditions. The temperature for the substrate was fixed at 580 ℃ during growth. The Be doping concentration is determined by the temperature of Be furnace. The former, labeled as sample A, has a constant Be concentration of 9.8×10^{18} cm^{-3} and a thickness of 1μm. The latter, labeled as sample B, consists of four layers of Be-doped GaAs with a thickness of 0.25μm for each layer. The Be concentrations, from the first layer to the fourth layer, are 1×10^{19}, 7×10^{18}, 4×10^{18}, and 1×10^{18} cm^{-3}, respectively. Each sample was divided into small pieces in size of 1.2cm × 1.2cm. The small pieces were used for activation.

The small pieces had to be treated before they were transferred to the activation system. First they were degreased by carbon tetrachloride, acetone, ethanol, and distilled water[12], and then rinsed in 1 ∶1 HF solution with the aim of removing surface oxide. Finally, the pieces were flushed using distilled water, made dry and quickly loaded into the vacuum system.

Figure 1 is the block diagram of our system. The system consists of three parts, including the surface analysis, the activation, and the evaluation. The pieces were first transferred to the heat cleaning chamber. The base pressure was below 7.5×10^{-8} Pa before each heat cleaning. To complete cleaning, we judged the surface cleanse degree by X-ray photoelectron spectrometer (XPS). The XPS spectra were measured in a Perkin-Elmer PHI ESCA 5300 spectrometer with an Al Kα X-ray beam. No sign of carbon was detected, indicating that a clean GaAs surface was obtained in the system. Then the pieces were moved to the activation chamber with a pressure below 1.2×10^{-7} Pa. The activation experiments for NEA photocathodes in the reflection mode were carried out by twice employing the ‘Yo-Yo’ technique[3,10,11,13~15]. Cs and O were alternatively injected on the clean GaAs surface at room temperature during the ‘Yo-Yo’ activation, and then the NEA surface was formed. The first ‘Yo-Yo’ activation was performed after the high temperature cleaning at 600 ℃ for 1h, and the second after the low temperature cleaning at 580 ℃ for 1h. A halogen tungsten filament lamp with 12V/50W was used to irradiate the photocathode surface throughout the whole activation process. The photoemission performance was evaluated by the on-line spectral response measurement system[16~20] when the activation process was finished.

For the time-resolved PL, the Ti: sapphire mode-locked laser was used as an excitation light source and the time-resolved PL spectra were measured using a streak camera (Hamamatsu Photonics C4334-02) with a 25cm polychromator (Hamamatsu Photonics C5094). The limit of the instrumental response of the system is to an exponential decay-time constant of approximately 15ps.

Raman scattering is a powerful tool to study the structure, chemical composition, orientation,

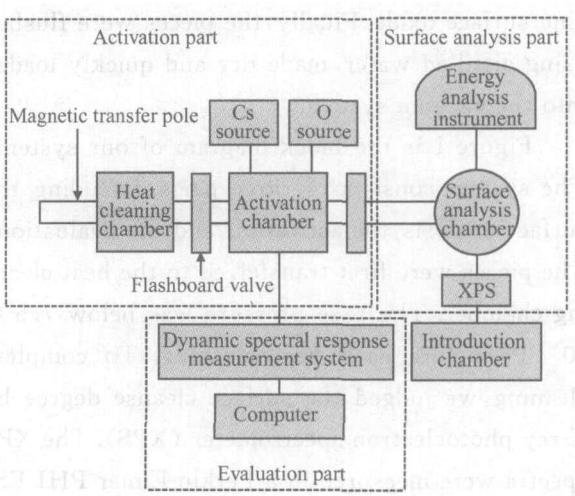

Fig. 1 Block diagram of the activation system

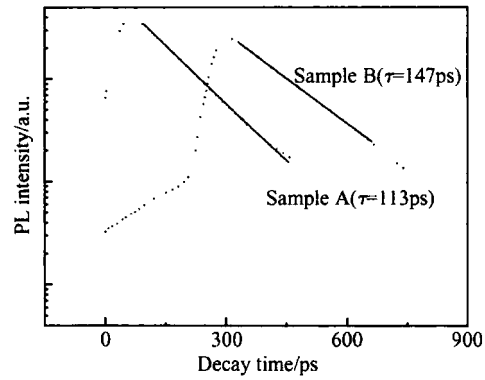

Fig. 2 PL decay curves of the dominant emission peaks for samples A and B at 10 K Dot lines represent the experimental data while solid lines show the single exponential fitting results.

and defects in semiconductor materials[21]. Probing the lattice vibration modes by Raman spectroscopy provides insight into the properties of GaAs epilayers as the normal penetration depth of the Ar^+ laser is approximately 100nm in crystalline GaAs[22].

Room temperature Raman scattering was characterized in the backscattering configuration with the 532nm line of an Ar^+ laser. The scattered light has been analyzed by a spectrometer with master 1800 grooves/mm holographic gratings and detected with a cooled CCD detector. The spot diameter of the focused laser beam on the sample is about 1μm. The resolution of the instrument is about 1.8cm^{-1}, and the unrepeatable error is within ±0.2cm^{-1}.

3 Results and discussion

The PL decay curves at 10K for samples A and B are shown in Fig. 2. The dot lines represent the experimental data while the solid lines indicate a single-exponential decay correspondent to the data. The decay-time constants are 113ps and 147ps for samples A and B, respectively. There is an increase of ~30% in the minority carrier lifetime. The longer PL lifetime indicates longer diffusion length in sample B.

Figure 3 shows the Raman spectra for samples A and B after growth and after activation, respectively, together with that of SI-GaAs substrate. The central frequency of the longitudinal optical (LO) phonon line for GaAs substrate is at 293.0cm^{-1} with a full width at half maximum (FWHM) of 5.11cm^{-1}. The almost symmetric shape of the LO line indicates that the SI-GaAs substrate can be treated as a bulk GaAs without much As precipitates[21]. The peak at 268.4cm^{-1} corresponds to the transverse optical (TO) phonon of GaAs. As a result of the backscattering configuration, only the LO phonon is allowed and the TO phonon is forbidden for the (001) oriented GaAs surface. Breaking of the selection rules[23~25] could be due to structural disorder[24] in the samples, and carbon contamination at the surfaces[26].

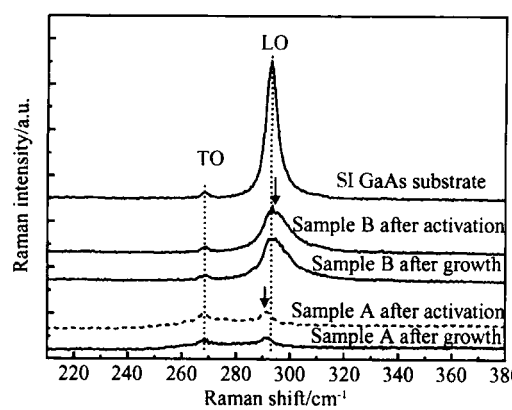

Fig. 3 Room temperature Raman spectra for samples A and B after growth and after activation, accompanied with that of SI-GaAs substrate in the backscattering geometry

For sample B, there is a very distinct LO peak and a low intensity TO peak. As a comparison, a weak LO peak with a comparable intensity TO line is present for sample A. The intensities ratio of the LO and TO phonons (I_{LO}/I_{TO}) is ~10 for sample B, ~1 for sample A, and ~30 for the SI-GaAs substrate, respectively. This demonstrates that there is a greater improvement in crystal quality in the case of sample B, though the degree of lattice perfection in each sample is inferior to that of the SI-GaAs substrate because the radius of the Be atom is smaller than that of the Ga atom.

Compared with the bulk GaAs, the LO phonon of samples A and B shifted to 291.0 cm^{-1} and 294.0 cm^{-1}, respectively, while the TO phonon at 268.4 cm^{-1} was almost unchanged for each sample. It can be deduced that there exists tensile stress in sample A and compressive stress in sample B. The difference in strain situation for samples A and B can be due to the effect of Be atom on the GaAs lattice structure. The lattice constant of Be-doped GaAs is smaller than that of the bulk GaAs because the Be atom has a smaller radius than the Ga atom. Therefore, tensile stress exists in Be-doped GaAs epilayer grown on SI-GaAs substrate. This is the case for sample A. In the case of sample B, underneath each layer was a heavily Be-doped GaAs layer, except for the SI-GaAs substrate. The top layer with Be concentration of 1×10^{18} cm^{-3} was grown on a layer with Be concentration of 4×10^{18} cm^{-3}. The Raman result indicates strain information for the top layer because the thickness of the top layer (0.25μm) is thicker than the penetration depth (~100nm) of the Ar^{+} laser. Accordingly, it is understandable to observe an apparent compressive strain for sample B. Note that the TO line becomes asymmetry in samples A and B when compared with that of the GaAs substrate. The asymmetry demonstrates that Be atom contributes to the lattice disorder of GaAs to a large extent.

No obvious Raman shift and intensity change can be found for each sample after growth and after activation, which can be explained by the experimental process. The Cs:O activated surfaces would disappear when the samples, after activation, were moved out of the ultra high vacuum system because Cs desorbed from the GaAs surface. The high (low) temperature cleaning can be regarded as an action of annealing. The GaAs epilayer was homoepitaxially grown on SI-GaAs substrate. Thermal annealing has a small effect on the homoepitaxial samples.

Two representative spectral response spectra for samples A and B are shown in Figs. 4(a) and (b) respectively. Note that no index definition has

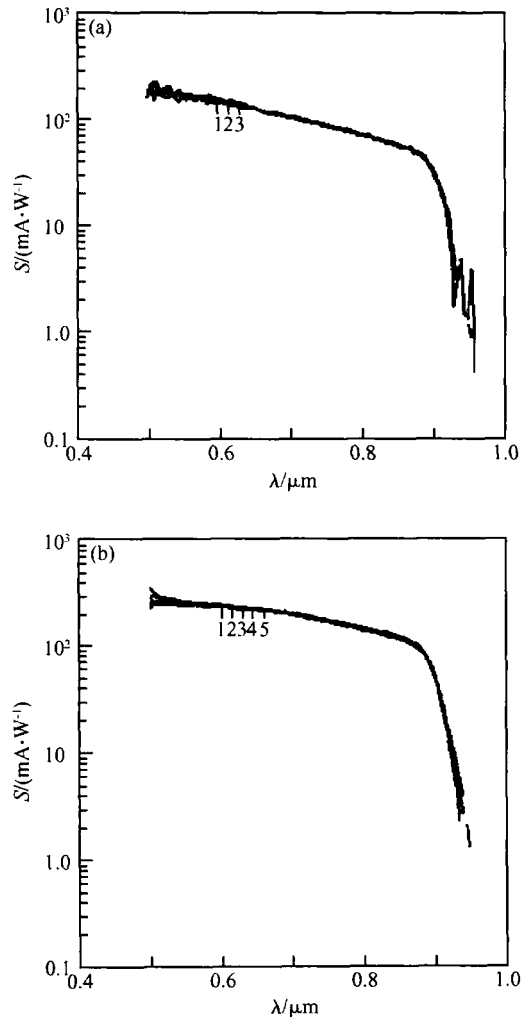

Fig. 4　(a) Spectral response spectra measured for one piece of sample A after the 'Yo-Yo' activation. The averaged integrated photosensitivity is 1039μA/lm; (b) Spectral response spectra measured for one piece of sample B after the 'Yo-Yo' activation. The averaged integrated photosensitivity is 1760μA/lm.

been put forward to evaluate the spectral response property in the past literature, and the reported sensitivity values were blow 100mA/W[27~29]. We define 100mA/W as the limit of high or low spectral response. A higher sensitivity value within a broad wavelength range is expected for photocathodes with a longer minority carrier diffusion length and a greater emission probability.

Figure 4(a) shows the spectral response spectra for one piece of sample A after the 'Yo-Yo' activation. The integrated sensitivity property was measured three times and with an average value of 1039μA/lm. The curves show a slightly linear decrease from 0.50μm up to ~0.90μm and then a dramatic reduction. Only when the wavelength is less than 0.72μm the spectral response is beyond 100mA/W. Figure 4(b) shows the online spectral response spectra for one piece of sample B after the 'Yo-Yo' activation. Five curves were collected to give an averaged integrated sensitivity value of 1760μA/lm, much higher than that for sample A. The shape of Fig. 4(b) is similar to that of Fig. 4(a). However, the wavelength is extended to 0.87μm before the sensitivity value decreases below 100mA/W in Fig. 4(b), indicating a prominent increase in infrared response.

Figure 5 shows the average integrated sensitivity results for five small pieces of samples A and B. The values range from 900 to 1200μA/lm for sample A and from 1550 to 1780μA/lm for sample B, indicating an increase of at least 50 %. The amount of error caused by the drift of the activation conditions is within 10 % for sample A and 5 % for sample B, which is much less than the increase of at least 50 % in the integrated sensitivity. We attribute the lower non-repeatable error in the case of sample B to the increase of the integrated sensitivity values.

The spectral response properties of NEA photocathodes are mainly affected by two main factors, the minority carrier diffusion length and the surface escape probability. Quantum efficiency is adopted to quantitatively evaluate the effect of the

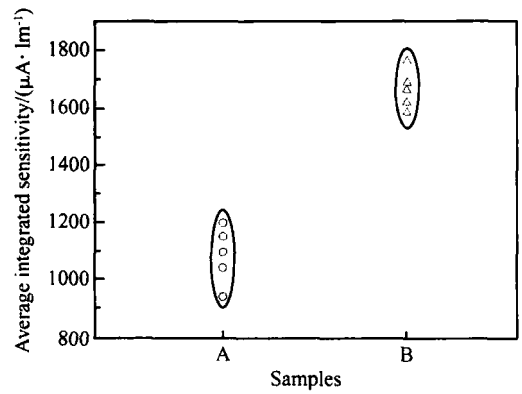

Fig. 5 Average integrated sensitivity results for five small pieces of samples A and B

two factors on integrated sensitivity. From the quantum efficiency equation in reflection mode[30], quantum efficiency is positively proportional to the minority carrier diffusion length and the surface escape probability. The ~30 % increase in the minority carrier lifetime means a corresponding increase of ~14 % in the minority carrier diffusion length. Therefore, the increase in the surface escape probability is about 32 % as the integrated sensitivity increases by ~50 %. This prompts us to deduce that, the increased spectral response in sample B should be due to the increase in the surface escape probability to a large degree and to the increase in the lifetime to a small degree.

However, the above-mentioned deduction seemingly contradicts with the view that the surface escape probability decreases with decreasing the acceptor concentration as a result of the broadening of the band bending region. The contradiction can be explained by considering the effect of the BSF-like structure. The intrinsic electric field generated by the concentration gradient exerts a force on photoelectrons, driving them to the surface. The extra drift velocity supplies energy to electrons and compensates the energy loss during the diffusion process to a degree. Additionally, the lattice and impurity scattering is weak in the multiplayer structure, as confirmed by the results of the PL decay spectra. When these positive effects prevail over the negative effect resulting from the broade-

ning of the band-bending region, the final effect is that photoelectrons with higher average energy diffuse to the surface and tunnel through the interfacial potential spike with higher probability.

In the analysis above, we assume that the change in the distribution of the Be-doping concentration has minor influence on the parameters, such as front (back) interface recombination velocity, surface reflectivity, and thickness and composition of the activated Cs-O layer. However, the Raman results indicate that compressive stress was observed in sample B, while tensile stress was observed in sample A. Here we could not estimate the relationship between the surface stress situation and the surface escape probability. Further investigation of this relationship will be conducted. Anyway, our work demonstrates that the BSF-like structure is an effective method for fabricating NEA GaAs photocathodes with higher integrated sensitivity if the multiplayer structure is to be optimized.

4 Conclusion

As a conclusion, we present investigations on the effect of sample structure on the photoelectronic performance of NEA GaAs photocathodes. It is found that the integrated photosensitivity can increase by at least 50 % by changing the Be concentration of the GaAs layer. The cause is attributed to the improvement in the crystal quality and the increase of the surface escape probability, especially the latter. These results suggest that higher integrated photosensitivity NEA GaAs photocathodes can be obtained by optimizing the distribution of Be concentrations in the GaAs layer.

Acknowledgment The authors would like to thank Yang X. D. at the Institute of Semiconductors, the Chinese Academy of Sciences and Liu Y. L. at the Institute of Physics, the Chinese Academy of Sciences for their help in PL and Raman measurements, respectively.

References

[1] Alley R, Aoyagi H, Clendenin J, et al. Stanford linear accelerator polarized electron source. Nucl Instrum Methods Phys Res A, 1995, 365: 1

[2] Yan Jinliang, Xiang Shiming. Studies of glass-bonded GaAs transmission photocathode by double crystal X-ray diffraction. Chinese Journal of Semiconductors, 1998, 19(9): 678 (in Chinese) [闫金良, 向世明. 透射式 GaAs 阴极粘接工艺的 X 射线双晶衍射研究. 半导体学报, 1998, 19(9): 678]

[3] Spicer W E. Negative affinity 3-5 photocathodes: their physics and technology. Appl Phys, 1977, 12(2): 115

[4] Bell R L. Negative electron affinity devices. Oxford: Clarendon Press, 1973

[5] Kamaratos M, Bauer E. Interaction of Cs with the GaAs(100) surface. J Appl Phys, 1991, 70(12): 7564

[6] Wang Liming, Cheng Zhao, Ping Qi, et al. Three-photon photoemission from GaAs-O-Cs negative electron affinity surfaces induced by 2.06μm nanosecond laser pulses. Appl Phys Lett, 1995, 67(1): 91

[7] Vergara G, Gomez A Herrera, Spicer W E. Electron transverse energy distribution in GaAs negative electron affinity cathodes: calculations compared to experiments. J Appl Phys, 1996, 80(3): 1809

[8] Weigel U, Orlov D A, Kosolobov S N, et al. Cold intense electron beams from LN2-cooled GaAs-photocathodes. Nuclear Instruments and Methods in Physics Research, Section A: Accelerators, Spectrometers, Detectors and Associated Equipment, 2005, 536(3): 323

[9] Chopra K L, Das S R. Thin film solar cells. New York: Plenum Press, 1983

[10] Fu Rongguo, Chang Benkang, Qian Yunsheng, et al. The evaluation system of negative electron affinity photocathode. Proc SPIE, 2001, 4580: 614.

[11] Zong Zhiyuan, Qian Yunsheng, Chang Benkang. A study on the activation technique of GaAs: Cs-O NEA photocathodes. Proc SPIE, 2003, 4796: 41

[12] Zong Zhiyuan, Qian Yunsheng, Chang Benkang. Analysis of on-line measured spectral responses of NEA photocathodes. Proc SPIE, 2001, 4580: 623

[13] Pierce D T, Meier F. Photoemission of spin-polarized electrons from GaAs. Phys Rev B, 1976, 13: 5484

[14] Fisher D G. Effect of Cs-O activation temperature on the surface escape probability of NEA (In, Ga) As photocathode. IEEE Trans Electron Devices, 1974, ED-21: 541.

[15] Laubschat C, Prietsch M, Domke M, et al. Switching of band bending at the nonreactive CsO_x/ GaAs(110) interface. Phys Rev Lett, 1989, 62: 1306

[16] Williams B F, Tietjien J J. Current status of negative electron

affinity devices. Proc IEEE ,1971 ,59(10) :1489.

[17] Su C Y ,Spicer W E ,Lindau I. Photoelectron spectroscopic determination of the structure of (Cs ,O) activated GaAs(110) surfaces. J Appl Phys ,1983 ,54(3) :1413

[18] Chang Benkang , Liu Wenli , Fu Rongguo , et al. Spectral response and surface layer thickness of GaAs :Cs-O negative electron affinity photocathode. Proc SPIE ,2001 ,4580 :632

[19] Chang Benkang ,Fang Hongbing ,Liu Yuanzhen. Invention patent of China ,1996 ,No. 94112317. 0

[20] Chang Benkang. Practically new-type patent of China ,2001 , No. 01237454. 0

[21] Zhang Fengyi , Tu Hailing , Wang Yonghong , et al. Study of As precipitates in LEC SI-GaAs wafer by Raman probe. Materials Science and Engineering B ,2000 ,75(2/3) :139

[22] Ishioka K ,Nakanura K G, Kitajima M. Phonon confinement in GaAs by defect formation studied by real-time Raman measurements. Phys Rev B ,1995 ,52 :2539

[23] Jimenz J , Gonzalez M A ,Martin B ,et al. Raman microprobe analysis of GaAs wafers. J Cryst Growth ,1990 ,103 :54

[24] Wang P D ,Cheng C , Sotomayer Torres C M ,et al. GaAs micrometer-sized dot imaging by Raman microscopy. J Appl Phys ,1993 ,74 :5907

[25] Pagès O ,Soltani M ,Zaoui A ,et al. A Raman study of coupled plasmon-LO phonon modes at ZnSe-GaAs interfaces. J Cryst Growth ,1998 ,184/185 :188

[26] Smanek R , Kinder R , Sciana B ,et al. Determination of doping profiles on bevelled GaAs structures by Raman spectroscopy. Appl Surf Sci ,2001 ,177 :139

[27] Qian Yunsheng , Zong Zhiyuan , Chang Benkang. Measurement of spectral response of photocathodes and its application. Proc SPIE ,2001 ,4580 :486

[28] Chang Benkang , Du Xiaoqing , Liu Lei ,et al. The automatic recording system of dynamic spectral response and its applications. Proc SPIE ,2003 ,5209 :209

[29] Chang Benkang , Fu Rongguo , Zong Zhiyuan , et al. On-line control for Cs-O layer thickness of NEA photocathode. Proc SPIE ,2003 ,4796 :33

[30] Sommer A H. Photoemissive materials preparation , properties ,and uses. John Wiley & Sons , Inc ,1968

高积分光电灵敏度多层 Be 浓度掺杂的 GaAs 负电子亲和势光电阴极

王晓峰[1] 曾一平[1] 王保强[1] 朱占平[1] 杜晓晴[2] 李 敏[2] 常本康[2]

(1 中国科学院半导体研究所 , 北京 100083)

(2 南京理工大学电子工程与光电子技术学院 , 南京 210094)

摘要: 研究了变掺杂浓度结构对 GaAs 负电子亲和势光电阴极积分光电灵敏度的影响. 通过 MBE 生长了两组 GaAs 同质外延样品. 其中一组采用了均匀掺杂的单层结构 ,Be 掺杂浓度为 $1\times10^{19}\,cm^{-3}$;另一组采用了变掺杂的多层结构 ,从衬底开始 Be 的掺杂浓度依次为 1×10^{19} ,7×10^{18} ,4×10^{18} 和 $1\times10^{18}\,cm^{-3}$. 负电子亲和势光电阴极通过在高真空系统中交替通入 Cs 和 O 激活得到. 在线光谱响应测试曲线表明 ,多层 Be 掺杂结构光阴极的积分光电灵敏度比单层 Be 掺杂结构光阴极的积分光电灵敏度至少提高了 50 %. 两种结构的 GaAs 样品表现出不同的表面应力情况.

关键词: 积分光电灵敏度; 多层结构; 负电子亲和势光电阴极; 扩散长度; 表面逸出几率

PACC: 3365; 7000; 6000

中图分类号: TN304. 2+3 **文献标识码**: A **文章编号**: 0253-4177(2005)09-1692-07

王晓峰 女 ,博士研究生 ,主要从事 GaAs 光电阴极材料与器件的研究. Email :xiaofw @red. semi. ac. cn

2005-02-21 收到 ,2005-04-12 定稿